

transmits 40% at 420 nm), using a 1000-W high-pressure mercury arc, destroyed only 60% of the T^+ in 30 min. Even if the matrix photolysis procedure is only 5% as effective as that used in the gas-phase experiments, photolysis of T^+ in the matrix is substantially less efficient than in the gas phase. The observed photochemical rearrangement of C^+ to T^+ also suggests a reduced rate of photodissociation for C^+ in the matrix. Since hydrogen atoms can diffuse freely through solid argon at 22 K without being retained by the matrix cage,³⁶ recombination of photolysis products in the matrix cage is an unlikely explanation for reduced photodissociation in the solid argon matrix. More likely, vibrational predissociation is rendered less effective in the matrix, owing to faster vibrational relaxation in the ground electronic state reached by internal conversion.

The matrix host provides an efficient sink for internal energy which is necessary to stabilize the T^+ and C^+ parent cations. Argon resonance radiation (11.6–11.8 eV) exceeds the threshold for production of $C_7H_7^+$ daughter ion from toluene (11.6 eV) and cycloheptatriene (10.1 eV),³⁷ however, the matrix quenches internal energy at a rate competitive with unimolecular decomposition and enables the parent cation to be stabilized. While internal energy is being quenched from the original parent cation formed, rearrangements of both T^+ and C^+ have been observed as C^+ was found in toluene studies (Figure 1a) and T^+ in cycloheptatriene experiments (Figure 1b).

The rearrangement of C^+ to T^+ on visible photolysis demonstrates that the balance between internal energy from visible light absorption by the ions and internal energy quenched by the matrix provides sufficient internal energy for rearrangement of the ions without dominant unimolecular decomposition. MINDO/3 calculations of the overall activation energy for $C^+ \rightarrow T^+$ rearrangement gave 39.8 and 39.2 kcal/mol (718 and 729 nm) for two different processes.³⁸ This is slightly lower than the first absorption detected at 542 nm, although the electronic band could tail additional vibrational quanta to the red. The matrix photolysis of C^+ with 750-nm radiation (38 kcal/mol) is in excellent agreement with the calculated activation energy for the $C^+ \rightarrow T^+$ isomerization. The observation of C^+ rearrangement with 750-nm photolysis at a finite rate in solid argon suggests that the activation energy for this rearrangement may in fact be somewhat

lower. An extensive progression in the C^+ absorption, probably involving the symmetric carbon-carbon ring breathing mode, indicates a geometry change on excitation; this structural change may aid the rearrangement process. Finally, the $C^+ \rightleftharpoons T^+$ isomerization documented here by optical spectroscopy provides support for the conclusion from gas-phase experiments^{10,15,16} that C^+ and T^+ are in equilibrium at relatively low internal energies.

Conclusions

The toluene and cycloheptatriene cations have been produced by argon resonance photoionization and trapped upon condensation at 22 K with excess argon. A 430-nm absorption in toluene experiments photolyzed with 420-nm cutoff light and is slightly red shifted from the 417-nm peak of the toluene ion PDS in the gas phase. Cycloheptatriene experiments produced a broad 480-nm absorption, near the 470-nm PDS peak for cycloheptatriene cation, and a small yield of the 430-nm absorption, which were clearly resolved. Visible photolysis *decreased* the 480-nm band and *increased* the 430-nm absorption, indicating that photochemical rearrangement of cycloheptatriene cation to toluene cation is competitive with photodissociation in these experiments.

The absorption spectroscopic observation of C^+ in toluene experiments and T^+ in cycloheptatriene studies supports the previously proposed equilibrium between C^+ and T^+ at relatively low internal energies. The toluene cation absorption bandwidth is more than an order of magnitude less in solid argon than in the gas phase. The sharper matrix band may be due to the absence of excess vibrational energy and/or a reduction in the rate of internal conversion from the excited state owing to efficient vibrational relaxation by the matrix. The slower photolysis rate for toluene cation in the matrix is consistent with the latter point and an efficient removal of vibrational excitation from the vibrationally hot ground state produced by internal conversion. The solid argon matrix is a useful medium for trapping large molecular ions for spectroscopic and photochemical studies under conditions where vibrational relaxation is a fast process. These matrix studies suggest that internal energy makes an important contribution to the bandwidth and photodissociation rate in ICR experiments.

Acknowledgments. The authors gratefully acknowledge financial support for this research from the National Science Foundation under Grant CHE 79-10966, helpful conversations with R. C. Dunbar, and the gift of samples from our organic colleagues and R. C. Dunbar.

(36) Smith, D. W.; Andrews, L. *J. Chem. Phys.* **1974**, *60*, 81.

(37) Rosenstock, H. M.; Draxl, K.; Steiner, B. W.; Herron, J. T. *J. Phys. Chem. Ref. Data, Suppl. 1* **1977**, *6*, 1-158.

(38) Dewar, M. J. S.; Landman, D. *J. Am. Chem. Soc.* **1977**, *99*, 2446.

Reactions of Fluorine with Methane upon Photolysis and Diffusion in Solid Argon. Infrared Spectra of HF Hydrogen-Bonded Complexes

Gary L. Johnson and Lester Andrews*

Contribution from the Chemistry Department, University of Virginia, Charlottesville, Virginia 22901. Received March 3, 1980

Abstract: Argon/methane and argon/fluorine samples were codeposited at 15 K. Mercury arc photolysis produced new absorptions assigned to the $CH_3F \cdots HF$ hydrogen-bonded complex characterized by an H-F stretching mode at 3774 cm^{-1} , significantly below the 3962-cm^{-1} isolated HF value, and a C-F stretching mode at 1003 cm^{-1} , also below the 1040-cm^{-1} CH_3F value. Sample warming to 25 K to allow diffusion and reaction of fluorine atoms produced additional new absorptions assigned to $H_3C \cdots HF$ characterized by an H-F stretching mode at 3764 cm^{-1} . The reaction of F atoms with CH_4 without radiation in solid argon at 25 K shows that this reaction requires practically zero activation energy.

Introduction

Fluorine reacts explosively with methane at room temperature; in fact, the low-pressure reaction of F_2 with $^{13}CH_4$ diluted in argon has been used to synthesize $^{13}CF_4$.¹ If, however, these reagents

are condensed in solid argon, the reaction requires photochemical initiation, and the products of one fluorine molecule and one

(1) Prochaska, F. T.; Andrews, L., unpublished results, 1976.

fluorine atom reacting with methane can be identified. The gas-phase reaction of photochemically produced fluorine atoms with methane gave vibrationally excited HF, the active medium in early chemical lasers.² Performing this reaction in a solid argon host provides a means of detecting both the HF and CH₃ radical products.

Jacox has reported an elegant study of fluorine atoms emerging from microwave discharged Ar/CF₄ or Ar/NF₃ and reacting with methane upon condensation at 14 K; the major products were identified as hydrogen-bonded complexes CH₃...HF and CH₃F...HF.³ The present complementary photochemical study of the F₂ and CH₄ reaction in solid argon provides several experimental advantages: (1) all extraneous absorptions in the sample can be identified before photolysis, (2) absorptions which appear on photolysis can be clearly observed, and (3) temperature cycling the sample to 25 K allows diffusion and further reaction of trapped fluorine atoms *without* light from a photolysis source.

The simple neutral hydrogen-bonded complexes CH₃...HF and CH₃F...HF are of considerable interest in their own right. In particular, a comparison of the H-F vibrational fundamental, ν_{HF} , in the complex provides a measure of the hydrogen-bond strength; increasing displacement below the 3962-cm⁻¹ value for HF in solid argon reveals increasing hydrogen-bond strength in the complex. The neutral π complex C₂H₂...HF exhibits a ν_{HF} at 3747 cm⁻¹;⁴ however, ν_{HF} appears substantially lower, 3562 cm⁻¹, in the charged complex (CF₂)⁻...HF,⁵ and in other charged complexes (CFX)⁻...HF (X = Cl, Br, I, and H) ν_{HF} ranges from 3456 to 3243 cm⁻¹,^{5,6} while for (CX₂)⁻...HF (X = Cl, Br), ν_{HF} = 3308 and 3287 cm⁻¹.⁷ The characterization of additional neutral HF complexes is needed to explore the utility of the H-F vibrational frequency as a probe for bonding in the complex.

Experimental Section

The cryogenic refrigeration system and vacuum apparatus have been described in detail previously.⁸ The Ar (Burdett, 99.995%), H₂ (Matheson), D₂ (Air Products), CH₄ (Matheson, research grade) and ¹³CH₄ and CD₄ (Merck Sharpe and Dohme) were all used as supplied without further purification. Fluorine (Matheson) at low pressure (<100 Torr) was passed through a 1/4 in. stainless-steel U-tube immersed in liquid N₂ into a stainless-steel vacuum system passivated overnight with F₂ at 100 torr. Argon/F₂ samples were deposited onto the cold window through a passivated 1/4 in. stainless-steel tube. Methyl fluoride (Matheson) was condensed at 77 K onto glass beads and distilled to remove volatile impurities before use. The HF used was produced by mixing equimolar amounts of F₂ and H₂ at low pressure in a 3-L stainless-steel can to produce 40 mmol of HF.

Samples of methane diluted 200/1 mol fraction and fluorine diluted 100/1 mol fraction with argon were used most frequently in this study. Methane diluted to 600/1, 300/1, 100/1, and 50/1 was also used along with F₂ dilutions of 300/1, 200/1 and 50/1 to investigate concentration effects. These samples were codeposited at rates of 3–4 mmol/h onto a CsI window at 15 K until 15 mmol of each sample was deposited. The resulting matrices were photolyzed for 1 h by the full light of a high-pressure mercury arc (Illumination Industries, Inc. BH-6-1, 1000 W) passed through a water filter. After spectra were recorded, the matrix was warmed to 25 K and then recooled to 15 K and further spectra were taken. Infrared spectra were recorded in the 4000–200-cm⁻¹ region on a Beckman IR-12 at ± 1 cm⁻¹ accuracy, and a Nicolet 7199 FT IR was used to take spectra with 0.5-cm⁻¹ resolution in the 4000–400-cm⁻¹ region.

Results

(CH₄ + F₂). Argon solutions of methane (Ar/CH₄ = 200/1) and fluorine (Ar/F₂ = 100/1) were codeposited onto a CsI window and the infrared spectrum was recorded; strong methane bands were observed at 3034 and 1306 cm⁻¹ and weak bands were observed at 3962, 1274, and 1024 cm⁻¹ from the usual HF, CF₄,

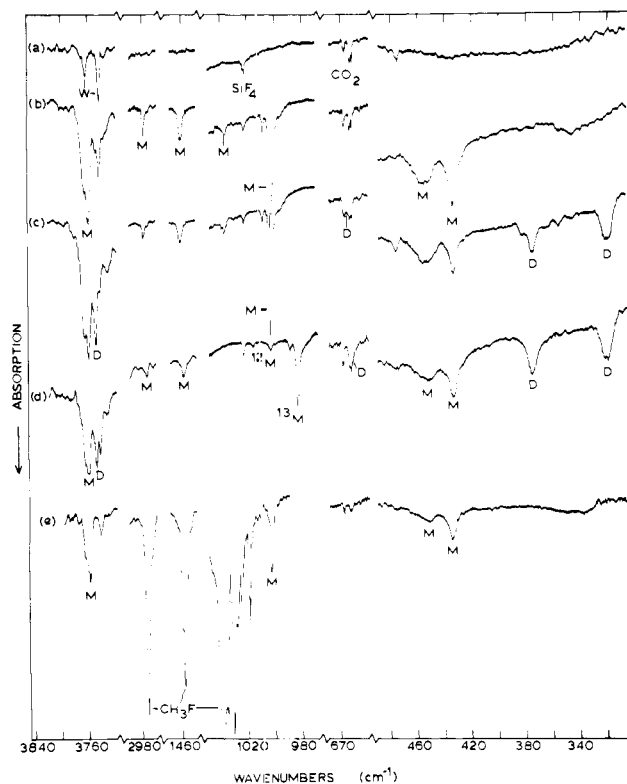


Figure 1. Infrared spectra of the argon/methane/fluorine reaction system at 15 K: (a) codeposited Ar/CH₄ = 200/1 and Ar/F₂ = 100/1 samples, W denotes water absorptions; (b) after 1.5 h mercury arc photolysis; (c) after warming to 25 K and cooling to 15 K; (d) Ar/¹³CH₄ = 100/1 and Ar/F₂ = 100/1 samples codeposited, photolyzed for 1 h, and cycled to 25 K; (e) Ar/CH₃F = 200/1 and Ar/HF = 100/1 samples codeposited at 15 K.

and SiF₄ impurities in fluorine. This sample spectrum is shown in Figure 1a for the regions of interest here. The matrix was then irradiated with the mercury arc lamp for 1 h, and further spectra were taken. Several new absorptions were observed after the photolysis of F₂ in the matrix; these bands are labeled M on trace (b) in Figure 1. A strong absorption in the HF region at 3774 cm⁻¹ with a weaker satellite at 3779 cm⁻¹ is of primary interest. Bands appeared at 2975, 1461, and 1038 cm⁻¹ near fundamental absorptions of CH₃F and a more prominent absorption was observed at 1003 cm⁻¹ with a satellite at 1009 cm⁻¹. The strongest of these bands, 1003 cm⁻¹, was observed by Jacox.³ A broad, moderately intense absorption centered at 455 cm⁻¹ and a sharper, more intense band at 435 cm⁻¹ always appeared with the same relative intensities despite efforts to separate them by independently varying the concentrations of the methane and fluorine.

After irradiation, the matrix was temperature cycled to 25 K to allow limited diffusion of trapped species, and further spectra were recorded. The bands formed by irradiation of the matrix changed only slightly in intensity after the diffusion cycle while several new absorption bands were produced; these bands are labeled D on trace (c) in Figure 1. A strong new absorption in the HF region at 3764 cm⁻¹ is the most prominent of the new bands. The remaining new absorptions consisted of a weak band at 666 cm⁻¹ between the two CO₂ bands, observed by Jacox,³ two broad absorptions centered at 377 and 323 cm⁻¹, and the strongest absorption of O₂F at 1489 cm⁻¹.⁹

The methane-fluorine experiments were repeated several times, using various concentrations of both fluorine and methane in order to study the concentration effects upon the relative intensities of the absorptions of the primary and secondary products. The majority of experiments were performed with Ar/CH₄ = 200/1 and Ar/F₂ = 100/1, but concentrations ranging from Ar/CH₄ = 600/1 to 50/1 and Ar/F₂ = 300/1 to 50/1 were also used. No

(2) Parker, J. H.; Pimentel, G. C. *J. Chem. Phys.* **1968**, *48*, 5273; **1969**, *51*, 91.

(3) Jacox, M. E. *Chem. Phys.* **1979**, *42*, 133.

(4) McDonald, S. A.; Johnson, G. L.; Keelan, B. W.; Andrews, L. *J. Am. Chem. Soc.*, **1980**, *102*, 2892.

(5) Andrews, L.; Prochaska, F. T. *J. Phys. Chem.* **1979**, *83*, 824.

(6) Andrews, L.; Prochaska, F. T. *J. Chem. Phys.* **1979**, *70*, 4714.

(7) Keelan, B. W.; Andrews, L. *J. Phys. Chem.* **1979**, *83*, 2488.

(8) Andrews, L. *J. Chem. Phys.* **1971**, *54*, 4935.

(9) Arkell, A. *J. Am. Chem. Soc.* **1965**, *87*, 4057.

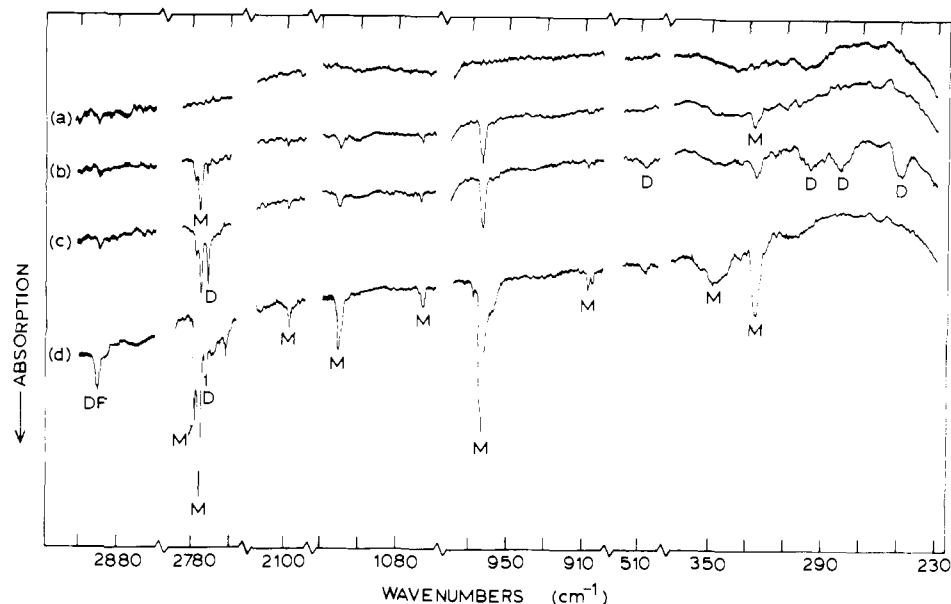


Figure 2. Infrared spectra of Ar/CD₄/F₂ samples at 15 K: (a) Ar/CD₄ = 50/1 and Ar/F₂ = 200/1 codeposited at 15 K; (b) after 1 h mercury arc photolysis; (c) after warming to 25 K and cooling to 15 K; (d) Ar/CD₄ = 100/1 and Ar/F₂ = 100/1 codeposited at 15 K and subjected to 30 min mercury arc photolysis.

changes in the relative intensities of the several M and D absorptions were observed through this study, nor were the relative yields of the M and D bands affected.

(¹³CH₄ + F₂). A repetition of the previously described experiment was performed by using methane-¹³C (Ar/¹³CH₄ = 100/1) and fluorine (Ar/F₂ = 100/1) in order to determine which bands showed carbon-13 shifts. After the matrix was irradiated, several new absorption bands were observed; these are labeled M on trace (d) in Figure 1. An intense absorption at 3774 cm⁻¹ and a weaker companion at 3779 cm⁻¹ are the bands of interest in the HF region. Also of interest are the two weak bands at 2970 and 1459 cm⁻¹ as well as the intense absorption at 983 cm⁻¹ with a weak satellite at 989 cm⁻¹, which occur near fundamental absorptions of ¹³CH₃F. A moderately strong absorption at 434 cm⁻¹ with a broad partner centered at 453 cm⁻¹ was also observed.

After the diffusion cycle the M absorptions produced by irradiation did not change significantly, while several new absorptions, labeled D on trace (d) in Figure 1, were observed. A strong new band appeared at 3764 cm⁻¹ in the HF region. A weak shoulder grew in at 661 cm⁻¹ on the CO₂ band and two moderately intense bands appeared at 376 and 321 cm⁻¹.

Another experiment with Ar/¹³CH₄ = 600/1 and Ar/F₂ = 50/1 gave essentially the same results on photolysis and diffusion.

(CD₄ + F₂). Additional isotope studies were performed by using methane-*d*₄ to determine deuterium shifts of the product absorptions. Spectra recorded after sample deposition in two experiments showed little reaction of CD₄ and F₂ during condensation, as evidenced by the weak DF absorption at 2896 cm⁻¹ (*A* = 0.02 and 0.04) in Figure 2. Spectra taken after the matrix was irradiated exhibited new absorptions, labeled M on traces (b) and (d) in Figure 2, from two experiments with different reagent concentrations. The new absorptions consisted of a moderately strong band in the DF region at 2767 cm⁻¹ with a weaker satellite at 2772 cm⁻¹, weak bands at 2094, 1111, and 1067 cm⁻¹, a moderately strong band at 964 cm⁻¹, a weak band at 908 cm⁻¹, and a moderately weak absorption at 326 cm⁻¹ with a broad satellite at 347 cm⁻¹. Band intensities are given in Table I for the two-step process shown in traces (b) and (c); however, the product bands were substantially stronger in the experiment illustrated in trace (d) of Figure 2.

After irradiation the matrix was warmed through a diffusion cycle and more spectra were recorded. The intensities of the absorption bands produced by photolysis were not significantly altered while several new absorptions, labeled D in trace (c) in Figure 2, were produced. The new absorptions consisted of a moderately strong peak at 2759 cm⁻¹, a weak absorption at 511

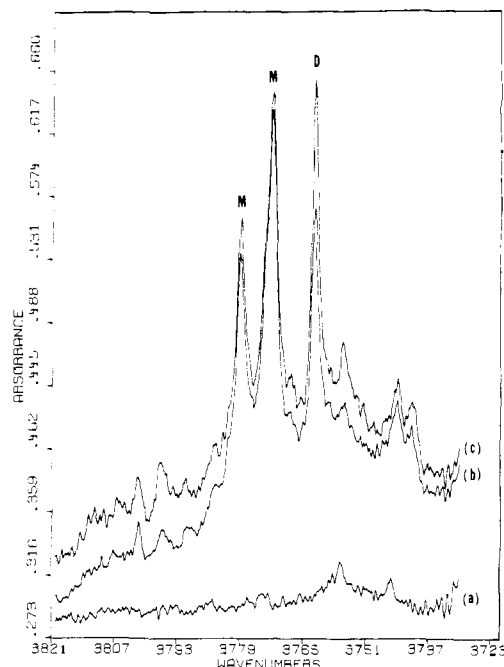


Figure 3. Infrared spectra of Ar/CH₄ = 100/1 and Ar/F₂ = 100/1 samples codeposited at 20 K using Nicolet FT IR shown in trace (a). Scan (b) recorded after 30 min mercury arc photolysis at 25 K. Trace (c) taken after sample warming to 34 K and cooling to 20 K.

cm⁻¹, and three moderately weak absorptions centered at 298, 281, and 249 cm⁻¹.

(CH₃F + HF). In order to provide more information on the absorptions arising from irradiation of the matrix, an experiment was performed with methyl fluoride (Ar/CH₃F = 200/1) and HF (Ar/HF = 100/1). The samples of CH₃F and HF were codeposited upon a CsI window at 15 K and spectra were taken. Product absorptions not due to CH₃F itself, labeled M on trace (e) of Figure 1, were observed at 3774 (with a shoulder at 3779), 1003, and 435 cm⁻¹ with a broad satellite at 453 cm⁻¹. It is clear that these absorptions correspond to the M bands resulting from photolysis of F₂ in the matrix.

One experiment was performed by using a Nicolet 7199 FT IR to record the spectra in order to compare the results to those obtained from a Beckman IR-12. Figure 3 shows the results of an experiment with Ar/CH₄ = 100/1 and Ar/F₂ = 100/1 on a

Table I. Absorption Bands (cm^{-1}) and Intensities (Absorbance Units) in Experiments Where Argon/Methane/Fluorine Samples at 15 K Were Subjected to Mercury Arc Photolysis Followed by Warming to 25 K

$\text{CH}_4 + \text{F}_2$		$^{13}\text{CH}_4 + \text{F}_2$		$\text{CD}_4 + \text{F}_2$		$\text{CH}_3 + \text{HF}$	ident
$h\nu$	25 K	$h\nu$	25 K	$h\nu$	25 K		
3962 (0.10)		3962 (0.11)		3962 (0.12)		3962 (0.13)	HF
3955 (0.06)		3955 (0.07)		3955 (0.07)		3955 (0.08)	HF
3779 (0.21)		3779 (0.14)				3779 (0.09)	M
3774 (0.35)		3774 (0.15)				3775 (0.14)	M
	3764 (0.11)		3764 (0.15)				D
3758 (0.08)		3758 (0.17)		3758 (0.10)		3758 (0.04)	H_2O
						3723 (0.05)	H_2O
							M
2975 (0.05)		2970 (0.02)				2969 (0.77)	CH_3F
				2896 (0.04)			DF
				2772 (0.03)			M
				2767 (0.07)			M
					2759 (0.09)		D
				2094 (0.01)			M
	1489 (0.02)		1489 (0.03)		1489 (0.02)		O_2F
						1465 (0.55)	CH_3F
1461 (0.06)		1459 (0.03)					M
				1111 (0.02)			M
				1067 (0.01)			M
						1040 (>0.9)	CH_3F
1038 (0.03)		1018 (0.02)					CH_3F
1009 (0.03)							M
1003 (0.32)		1003 (0.01)				1003 (0.199)	M
		989 (0.01)					M
		983 (0.10)					M
				964 (0.06)			M
				908 (0.01)			M
	669 (0.03)		669 (0.04)				CO_2 (g)
	666 (0.03)						D
							CO_2
	664 (0.02)		664 (0.05)				CO_2
			662 (0.06)				D
			661 (0.02)		511 (0.01)		
		476 (0.06)					M
455 (0.06)		453 (0.05)				453 (0.03)	M
435 (0.14)		434 (0.07)				435 (0.06)	M
	377 (0.05)		376 (0.09)				D
	323 (0.06)		322 (0.03)				D
				347 (0.01)			M
				326 (0.03)			M
					298 (0.03)		D
					281 (0.04)		D
					249 (0.04)		D

20 K substrate in the 3720–3820- cm^{-1} region. Trace (b) shows the results after 30 min of irradiation, and trace (c) shows the effect of warming the matrix to 34 K and cooling back to 20 K. The absorptions at 3772 and 3779 cm^{-1} in trace (b) are better resolved while the absorption at 3763 cm^{-1} was produced due to warming of the matrix to 25 K during irradiation; this band increased on sample warming to 34 K, as shown in trace (c). One of the advantages of the FT IR is its ability to ratio out background absorptions due to water in the matrix, which can be seen by comparing the same regions in Figures 1 and 3.

Discussion

In a preceding study new absorptions at 664, 1003, and 3764 cm^{-1} produced by reaction of methane and fluorine atoms from microwave discharge of CF_4 or NF_3 in argon were assigned to the hydrogen-bonded species $\text{CH}_3\cdots\text{HF}$ and $\text{CH}_3\text{F}\cdots\text{HF}$.³ The spectra resulting from this procedure are complicated by CF_4 or NF_3 byproducts, as well as the fact that the primary and secondary products are formed simultaneously. The method reported in the present study provides a simpler way to observe the spectra of the two products; the use of F_2 eliminates any byproducts from the generation of F atoms, and the two-step process first forms the two-fluorine product $\text{CH}_3\text{F}\cdots\text{HF}$ by irradiation, and then diffusion gives the single-fluorine species, $\text{CH}_3\cdots\text{HF}$, clearly demonstrating that two different products are formed.

($\text{CH}_3\text{F}\cdots\text{HF}$). The three strong bands appearing upon mercury arc photolysis in the present study, labeled M at 3774, 1003, and 435 cm^{-1} , were also produced upon codeposition of argon samples

of CH_3F and HF. This conclusively shows that these M bands are due to the $\text{CH}_3\text{F}\cdots\text{HF}$ hydrogen-bonded complex, suggested by Jacox³ to explain the strongest band at 1003 cm^{-1} . This also confirms the conclusion of Jacox that the 3764- cm^{-1} band, labeled D in the present studies, is due to a different hydrogen-bonded complex, $\text{CH}_3\cdots\text{HF}$, to be discussed in the next section.

The M bands at 3774 and 3779 cm^{-1} are assigned to the H-F stretching mode of the $\text{CH}_3\text{F}\cdots\text{HF}$ complex presumably split by different matrix trapping sites. These bands are appropriately displaced from the isolated HF fundamental at 3962 cm^{-1} in solid argon, and they are near the 3747- and 3732- cm^{-1} values of $\nu_{\text{H-F}}$ for the π complexes $\text{C}_2\text{H}_2\cdots\text{HF}$ and $\text{C}_2\text{H}_4\cdots\text{HF}$.⁴ This assignment is consistent with the observed deuterium shift to a 2767, 2772 cm^{-1} doublet, H/D = 1.364, and the absence of any detectable carbon-13 shift. The observed ratio for matrix-isolated HF and DF is 3962/2896 = 1.368, which is almost identical.

The fundamental absorption bands of CH_3F , $^{13}\text{CH}_3\text{F}$, and CD_3F are compared to the bands observed after the photolysis of F_2 with CH_4 , $^{13}\text{CH}_4$, and CD_4 in Table II. The ν_3 mode of CH_3F was perturbed the most by HF with a red shift of 37 cm^{-1} , which indicates that the hydrogen bond is directed toward the fluorine atom of CH_3F . The ν_2 mode was red shifted only 2 cm^{-1} by the HF perturbation, probably due to a small increase in the reduced mass of the C-F portion of the molecule when the HF is hydrogen bonded to the fluorine. The ν_1 mode of CH_3F was blue shifted by 6 cm^{-1} in the hydrogen-bonded species, which may be due to a slight increase in C-H bond strength. This could be caused by a reduction in the C-F bond strength owing to the $\text{H}_3\text{C-F}\cdots\text{H-F}$

Table II. Comparison of Isotopic Methyl Fluoride Fundamentals (cm^{-1}) with $\text{CH}_3\text{F}\cdots\text{HF}$ Fundamentals in Solid Argon at 15 K^a

	CH_3F	$\text{CH}_3\text{F} + \text{HF}$
$\nu_1(\text{a}_1)$	2969	2975
$\nu_2(\text{a}_1)$	1463	1461
$\nu_3(\text{a}_1)$	1040	1003
	$^{13}\text{CH}_3\text{F}$	$^{13}\text{CH}_3\text{F} + \text{HF}$
$\nu_1(\text{a}_1)$	2962	2970
$\nu_2(\text{a}_1)$	1461	1459
$\nu_3(\text{a}_1)$	1019	983
	CD_3F	$\text{CD}_3\text{F} + \text{DF}$
$\nu_1(\text{a}_1)$	2087	2094
$\nu_2(\text{a}_1)$	1128	1111
$\nu_3(\text{e})$	1069	1067
$\nu_3(\text{a}_1)$	989	964
$\nu_6(\text{e})$	912	908

^a E. S. Prochaska and L. Andrews, unpublished spectra of CH_3F , CD_3F , and $^{13}\text{CH}_3\text{F}$ in solid argon (1978).

hydrogen bond, which may increase the electron density the carbon has available to share with the hydrogens. A similar effect can be seen in the 8- cm^{-1} blue shift of the ν_1 mode going from CH_3F through CH_3Cl to CH_3Br .¹⁰ It is perhaps noteworthy that the symmetric vibrational modes of CH_3F are intensified by hydrogen bonding to HF more than the antisymmetric modes, some of which were seen only for the $\text{CD}_3\text{F}\cdots\text{DF}$ species.

The two remaining absorptions at 435 and 455 cm^{-1} are assigned to the deformation mode of the HF proton in the hydrogen-bonded species, with the splitting due to different orientations of the HF in the matrix. This is consistent with the deuterium shifts to 326, H/D = 1.334, and 347 cm^{-1} , H/D = 1.311, observed for the two absorptions. The decrease in the H/D ratios from ν_{HF} to the deformation mode, which is also seen in earlier work involving charged species,⁵⁻⁷ seems to be characteristic of this type of deformation mode. A very weak absorption at 1038 cm^{-1} is tentatively assigned to the 1040- cm^{-1} ν_3 fundamental of isolated CH_3F , but it could also be CH_3F perturbed by HF at an undertermined position.

($\text{CH}_3\cdots\text{HF}$). The new bands produced only by sample warming to allow diffusion of reactive species, labeled D at 3764, 666, 377, and 323 cm^{-1} , are assigned to the simple fluorine atom-methane reaction product $\text{H}_3\text{C}\cdots\text{HF}$, in agreement with Jacox (who observed only the two higher bands due to a 400- cm^{-1} instrumental limit).³

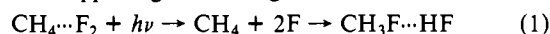
The sharp absorption band found at 3764 cm^{-1} after the diffusion cycle is assigned to the stretching mode of HF hydrogen bonded to methyl radical at the carbon. This assignment is supported by a deuterium shift to 2759 cm^{-1} , H/D = 1.364, for the perturbed HF as compared to an H/D ratio of 1.368 for unperturbed HF. The red shift of 10 cm^{-1} going from $\text{H}_3\text{CF}\cdots\text{HF}$ to $\text{H}_3\text{C}\cdots\text{HF}$ demonstrates that the unpaired electron on the methyl radical forms a stronger H bond than the fluorine on CH_3F ; i.e., the half-filled p orbital on the methyl radical is a better contributor of electron density to the hydrogen bond than a fluorine atom, which is to be expected. Since the hydrogen bond is stronger with the methyl radical than CH_3F , the possibility of the HF being bonded to one of the methyl-radical hydrogens can be discarded.

The weak band located at 666 cm^{-1} between the CO_2 bands is identified as the out-of-plane deformation of the perturbed methyl radical, found at 617 cm^{-1} in the unperturbed radical, as discussed by Jacox.^{3,11} In earlier work on the methyl radical,^{12,13} the presence of alkali iodides gave rise to a similar blue shift in the out-of-plane deformation mode of CH_3 . For the series CH_3 , $\text{CH}_3 + \text{HF}$, $\text{CH}_3 + \text{NaI}$, and $\text{CH}_3 + \text{LiI}$, the out-of-plane deformation mode is found at 617, 666, 696, and 730 cm^{-1} , re-

spectively, and the H/D ratios are 1.362, 1.303, 1.305, and 1.287. If ammonia is added to this series with a symmetric deformation at 974 cm^{-1} in solid argon¹⁴ and an H/D ratio of 1.285, and if it is assumed that methyl radical deforms from planarity more when bonded to the stronger ligand, then it is apparent that LiI forms stronger induced dipole associations than NaI, which in turn is a stronger ligand than HF.

The absorption band centered at 377 cm^{-1} is assigned to the deformation mode of the hydrogen-bonded hydrogen in the $\text{H}_3\text{C}\cdots\text{H-F}$ complex. The absorption at 323 cm^{-1} is probably due to the deformation mode for this complex with a different geometric orientation of the HF ligand and the methyl radical. Hydrogen deformation modes in a number of analogous HF complexes exhibit similar multiple absorptions.^{5,6} The 377- and 323- cm^{-1} bands exhibit 1- cm^{-1} carbon-13 shifts and large deuterium displacements, which is expected for a $\text{C}\cdots\text{H-F}$ bending mode; the H/D ratios for the 377- and 323- cm^{-1} absorptions are 1.342 and 1.297, respectively. It is also interesting to note that the $\text{H}_3\text{C}\cdots\text{HF}$ hydrogen bond is less rigid than the $\text{CH}_3\text{F}\cdots\text{HF}$ hydrogen bond, as shown by the higher deformation mode for the latter.

Reactions Occurring in the Matrix. The large yield of the two-fluorine species $\text{CH}_3\text{F}\cdots\text{HF}$ in these experiments indicates that $\text{CH}_3\text{F}\cdots\text{HF}$ is a primary photolysis product of $\text{CH}_4\cdots\text{F}_2$ van der Waals dimers trapped together during condensation of the matrix:



It is noteworthy that little reaction occurred during codeposition of these reagents, as very little isolated DF was observed in the $\text{CD}_4\text{-F}_2$ experiments. Since the single-fluorine species $\text{CH}_3\cdots\text{HF}$ was not observed upon photolysis, it is concluded that reaction 1 does not stabilize any $\text{CH}_3\cdots\text{HF}$ intermediate. However, on diffusion, fluorine atoms produced from isolated F_2 molecules react with methane, according to the reaction



as proposed by Jacox.³ It is noteworthy that reaction 2 can take place in solid argon at 25 K in the absence of light, indicating that hydrogen abstraction from hydrocarbons by atomic fluorine requires essentially no activation energy.

The experiments described here are nicely complementary to those of Jacox, where (2) was the primary reaction and $\text{CH}_3\cdots\text{HF}$ the major product, and $\text{CH}_3\cdots\text{HF}$ was formed by a second fluorine atom addition to $\text{CH}_3\cdots\text{HF}$. In the present photolysis experiments, $\text{CH}_3\text{F}\cdots\text{HF}$ is the major product and $\text{CH}_3\cdots\text{HF}$ is formed upon diffusion by reaction 2.

Hydrogen Bonding in HF Complexes. One goal of this study was to characterize neutral HF hydrogen-bonded complexes by their ν_{HF} mode. The 3774- and 3764- cm^{-1} values for $\text{CH}_3\text{F}\cdots\text{HF}$ and $\text{CH}_3\cdots\text{HF}$ involving hydrogen bonding to a fluorine lone pair and a carbon free radical center are near the 3747- and 3732- cm^{-1} values for the $\text{C}_2\text{H}_2\cdots\text{HF}$ and $\text{C}_2\text{H}_4\cdots\text{HF}$ π complexes.⁴ However, ν_{HF} absorptions in the 3200-3500- cm^{-1} region identified as haloform electron-capture products⁵⁻⁷ exhibit stronger hydrogen bonds. This is consistent with their anionic character since anions in general should exhibit substantially higher proton affinities than neutral molecules. The position of ν_{HF} , more specifically the displacement from the isolated HF value, provides a measure of hydrogen-bond strength and serves as a probe for electronic characterization of the hydrogen-bonding partner. For example, the largest H-F mode displacement (to 1377 cm^{-1})¹⁵ in a hydrogen-bonded species has been observed for the strongest hydrogen bond, in $(\text{F-H-F})^-$, which arises from the extremely high proton affinity of the fluoride ion.

Conclusions

The hydrogen-bonded complexes $\text{CH}_3\text{F}\cdots\text{HF}$ and $\text{H}_3\text{C}\cdots\text{HF}$ can be formed by the reaction between methane and fluorine atoms produced by photolytically cleaving F_2 in the matrix with fewer

(10) Herzberg, G. "Infrared and Raman Spectra"; Van Nostrand: Princeton, N.J., 1945.

(11) Jacox, M. E. *J. Mol. Spectrosc.* **1977**, *66*, 272.

(12) Andrews, L.; Pimentel, G. C. *J. Chem. Phys.* **1967**, *47*, 3637.

(13) Tan, L. Y.; Pimentel, G. C. *J. Chem. Phys.* **1968**, *48*, 5202.

(14) Milligan, D. E.; Hexter, R. M.; Dressler, K. *J. Chem. Phys.* **1961**, *34*, 1009.

(15) McDonald, S. A.; Andrews, L. *J. Chem. Phys.* **1979**, *70*, 3134.

complications than techniques using discharge sources of fluorine atoms. The $\text{CH}_3\text{F}\cdots\text{HF}$ product forms upon photolysis of a F_2 molecule adjacent to methane in the matrix, and the $\text{H}_3\text{C}\cdots\text{HF}$ product forms after diffusion and reaction of methane with free fluorine atoms. This two-step process conclusively shows that two different species are produced. The reactions of fluorine atoms

with methane in solid argon at 25 K show that this reaction requires virtually no activation energy.

Acknowledgments. The authors gratefully acknowledge financial support from the National Science Foundation under Grant CHE-79-10966.

Determination of the Basicities of Benzyl, Allyl, and *tert*-Butylpropargyl Anions by Anodic Oxidation of Organolithium Compounds

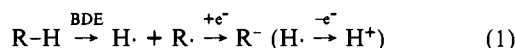
Bernhard Jaun, Joshua Schwarz, and Ronald Breslow*

Contribution from the Department of Chemistry, Columbia University, New York, New York 10027. Received March 31, 1980

Abstract: Electrochemical oxidation potentials have been determined by using cyclic voltammetry and second-harmonic ac voltammetry for benzylolithium, allyllithium, *tert*-butylpropargyllithium, and triphenylmethylolithium in tetrahydrofuran/hexamethylphosphoramide. The use of these potentials along with bond dissociation energies and the known $\text{p}K_a$ of triphenylmethane permit the estimation of ion-pair acidities of the corresponding hydrocarbons, expressed as $\text{p}K_a$'s. These are compared with other estimates for the $\text{p}K_a$ of toluene and with estimates of the $\text{p}K_a$'s of isobutane and methane. Electrochemical studies are also reported for diphenylmethylolithium, cyclopentadienyllithium, vinylolithium, phenyllithium, methylolithium, and *n*-butyllithium. The first two were well-behaved and permit us to calculate the $\text{p}K_a$ of cyclopentadiene and a bond dissociation energy for diphenylmethane. The others give electrochemistry so poor that it is useful only to estimate lower limits to the corresponding $\text{p}K_a$'s.

Introduction

We have described the use of electrochemical data to provide thermodynamic estimates of the basicities of a variety of carbanions.¹⁻⁷ The general validity of the approach was demonstrated by its ability to reproduce a number of directly determined equilibrium constants reflecting stabilities not only of carbanions but also of carbonium ions⁸ and of radicals.⁵ For hydrocarbon acidities the method⁶ is simple: the sequence of eq 1 is examined



for the unknown and for a known model compound. Using the bond dissociation energy (BDE) for each and the electrochemical reduction potential for each radical, it is straightforward to calculate the $\text{p}K_a$ of R-H from the known $\text{p}K_a$ of the model compound, assuming that it mirrors the other changes (e.g., from gas-phase BDE to solution electrochemistry) involved in the sequence. With this method we have determined⁶ the $\text{p}K_a$ of isobutane (forming a *tert*-butyl anion) to be 71.

It was shown⁷ that the result for isobutane is not very sensitive to the medium used for the electrochemistry, and in the same publication it was reported that in the electrochemical reduction of benzyl iodide, of allyl iodide, and of propargyl iodide there were two reduction waves, the second of which was assigned to reduction of the corresponding radicals to anions. Unfortunately, the "first wave" was actually a prewave due to adsorption of iodide on the metal electrodes and is not seen at vitreous carbon electrodes. This has been shown by Bard⁹ for allyl iodide, and we¹⁰ and Bartak¹¹

have shown it for benzyl iodide. Thus the "second wave" for benzyl, allyl, and propargyl was not for the one-electron reduction of carbon radicals to anions, and the $\text{p}K_a$'s derived from it are invalid. The $\text{p}K_a$'s of 54, 53, and 63 which were reported⁷ for the formation of benzyl, allyl, and propargyl anions are simply upper limits if the true reduction potential of the radicals is anodic of the potentials required to reduce the covalent iodides to carbanions. Our results described below will show that this is indeed the case. By contrast, we find that *tert*-butyl iodide shows the same two reduction waves at a vitreous carbon electrode as those we have described earlier⁶ at metal. Thus the complication in the previously reported electrochemistry of benzyl iodide, allyl iodide, and propargyl iodide is not present for *tert*-butyl iodide.

In principle the reduction potential for conversion of a radical to an anion is obtainable from the reverse process, oxidation of the anion.^{8,9} The experimental problem is to produce stable solutions of the appropriate carbanions for study. This can be approached by the use of organolithium species.⁸ Extensive studies have shown that compounds such as benzylolithium¹² and allyllithium,¹³ with delocalized carbanion components, do not have covalent carbon-lithium bonds but exist as carbanion-lithium ion pairs in solvents such as tetrahydrofuran (THF) or hexamethylphosphoramide (HMPA). The situation is less clear for lithio derivatives of less stable anions, as in methylolithium. Such species often exist as clusters,¹⁴ and the extent to which they can be thought of as containing methyl anion is problematical.

In order to obtain better electrochemical and $\text{p}K_a$ data, we have thus examined the anodic oxidation of benzylolithium (1) and of allyllithium (2). As an approximation to propargyllithium we have prepared and examined 1-lithio-4,4-dimethylpent-2-yne (*tert*-

(1) Breslow, R.; Balasubramanian, K. *J. Am. Chem. Soc.* **1969**, *91*, 5182-3.

(2) Breslow, R.; Chu, W. *J. Am. Chem. Soc.* **1970**, *92*, 2165.

(3) Breslow, R.; Chu, W. *J. Am. Chem. Soc.* **1973**, *95*, 411-8.

(4) Breslow, R. *Pure Appl. Chem.* **1974**, *40*, 493-509.

(5) Wasielewski, M. R.; Breslow, R. *J. Am. Chem. Soc.* **1976**, *98*, 4222-9.

(6) Breslow, R.; Goodin, R. *J. Am. Chem. Soc.* **1976**, *98*, 6076.

(7) Breslow, R.; Grant, J. *J. Am. Chem. Soc.* **1977**, *99*, 7745-6.

(8) Breslow, R.; Mazur, S. *J. Am. Chem. Soc.* **1973**, *95*, 584-5.

(9) Bard, A. J.; Merz, A. *J. Am. Chem. Soc.* **1979**, *101*, 2959-65.

(10) Reference 9, footnote 42.

(11) Reference 9, footnote 19.

(12) O'Brien, D. H.; Russell, C. R.; Hart, A. J. *J. Am. Chem. Soc.* **1979**, *101*, 633-9.

(13) Thompson, T. B.; Ford, W. T. *J. Am. Chem. Soc.* **1979**, *101*, 5459-64 and references therein.

(14) West, P.; Waack, R. *J. Am. Chem. Soc.* **1967**, *89*, 4395-9 and references therein.